Article

Journal of
Nanoscience and Nanotechnology
Vol. 17, 7061–7068, 2017
www.aspbs.com/jnn

Effect of Solvent on the γ-Aminopropyltriethoxysilane Modified Titanium-Pillared Montmorillonite

Dujuan Zhang[1,2], Zonghua Qin[1,*], Quan Wan[1], Shanshan Li[1,4], Yuhong Fu[1,3], Yuantao Gu[1,3], and Shuqin Yang[1]

[1] State Key Laboratory of Ore Deposit Geochemistry, Institute of Geochemistry, Chinese Academy of Sciences, Guiyang 550081, China
[2] School of Chemistry and Chemical Engineering, Guizhou University, Guiyang 550025, China
[3] University of Chinese Academy of Sciences, Beijing 100049, China
[4] School of Chemistry and Materials Science, Guizhou Normal University, Guiyang, Guizhou 550001, China

Titanium pillared montmorillonite was prepared by the sol–gel method with the precursor of isopropyl titanate. Subsequently, the Ti-pillared montmorillonite was modified by γ-aminopropyltriethoxysilane (APTES) in three solvents with different polarities. Combining with X-ray diffraction pattern, Fourier transform infrared spectroscopy, thermal analysis, scanning electron microscopy, and nitrogen adsorption–desorption, the structure, morphology, specific surface area, and pore-size distribution of the product were discussed. The distance of (001) lattice planes achieved 11.46 nm after titanium pillaring, accompanied with the increased specific surface area and pore size. The hydrolysis of APTES was easy to conduct in the presence of anhydrous ethanol and methanol. Since the water molecules on the surface of titanium oxide can be replaced by alcohol, the hydrolysis of APTES was promoted and the samples have high silane loading amounts in ethanol and methanol systems. However, due to the molecular repulsion, the water molecules tend to enter the interlayer channel of titanium pillared montmorillonite in cyclohexane system. This inhibited the bonding between silanes and interlayer titanium oxides, resulting in a lower grafted amount. Therefore, by choosing different solvents, the grafting amount of silane on the Ti-pillared surface could be adjusted.

Keywords: Montmorillonite, Titanium-Pillared, Solvents, γ-Ammoniapropyltriethoxysilane, Silyation.

1. INTRODUCTION

Montmorillonite is a kind of clay mineral with natural nanostructure, which is widely distributed and possesses many unique properties, such as cation exchange capacity, large specific surface area, dispersity and rheology. Therefore montmorillonite is widely used as adsorbent,[1] functional materials,[2] nanocomposite materials,[3–5] etc. Montmorillonite has a 2:1 layer structure and its structure unit consists of two tetrahedral sheets of $[SiO_4]$ and one octahedral sheets of $[AlO_2(OH)_4]$. Its interlayer space can be reshaped and the interlayer hydrated cation[6–9] can be exchanged, which results in good adsorption performance for heavy metal ion and cationic dyes.[10,11] However, pristine montmorillonite usually has some limitations, such as small interlayer spacing. In order to enlarge the application fields, montmorillonite usually need to be modified.

Early research commonly focused on a single-type modification, like inorganic pillaring and organic modification. For inorganic pillaring, metal cations intercalate into the interlayer spacing through ion exchange, and then are immobilized by calcination under a certain temperature.[12] Montmorillonite can obtain a larger interlayer spacing and specific surface area after inorganic pillaring. The intercalation of metal oxides could enhance the adsorption capacity, but its hydrophilic surface still restrains the removal of hydrophobic organic contaminants. For organic modification, surfactants are usually used in order to enhance the organic affinity. The cationic surfactant is exchanged into the interlayer space, making the surfaces hydrophilic and enhancing the adsorption capacity of organic pollutants. Since there is no stable bonding between cationic surfactant and montmorillonite, cationic surfactant can easily leach out with the fluctuation of pH and ionic strength, leading to secondary pollution.[5,13,14] In order to enhance the combination between organic matter and

*Author to whom correspondence should be addressed.

montmorillonite, researchers have used organic silane to modify montmorillonite. Organic silane can form covalent bonds with silanol (–SiOH), aluminol (–AlOH) in montmorillonite surface via hydrolysis, improving the stability of the organic montmorillonite.[15–18] In previous organic silane modification studies of clay minerals, toluene or organic solvent-aqueous solution were usually used as the reaction medium, and the concerns are mainly focused on the structure and adsorption capacity of the modified products. However, it received little attention for the effects of other reaction mediums on amount of grating and the manner of grafting.[4,19] The influence of different dispersion mediums for silane modified montmorillonite was proposed by Shanmugharaj.[20] There were investigations on the effects of γ-ammoniapropyltriethoxysilane to the modification of montmorillonite in different polar solvents (ethanol, toluene) to modify montmorillonite. Su et al. discussed the influence of polarity to the amount and behavior of silane grafting on montmorillonite and inspected the expansion process of the interlayer grafting product in different solvent.[21]

Meanwhile, some researchers conduct composite modification by combining the advantages of inorganic and organic modification of montmorillonite. Li et al. synthesized an inorganic–organic montmorillonite by using polyhydroxy-aluminum (iron) cations and cetyltrimethyl ammonium bromide (CTAB) and investigated its adsorption capacity for the herbicides 2,4-dichlorophenoxyacetic acid and acetochlor.[22] Al-Asheh et al. discussed the removal of phenol in aqueous solution with different types of activated bentonites, and compared the adsorption capacities of the pristine, single-modified (aluminum polyhydroxycations, CTAB, or cyclohexane) and composite-modified (CATB/Al) bentonite.[23] Although these composite materials combined the advantages of both inorganic and organic modified montmorillonite and had broad application prospects, its defect—the leakage of interlayer surfactant molecules with the changes of pH and ionic strength—was not actually overcome. In order to obtain more stable products, organosilanes were chosen to substitute these surfactants products. These novel organic–inorganic composites would have various properties by using the silanes with different functional groups, thus improving the adsorption capacity of targeted pollutants and obtaining nanocomposites with unique optical and electrical properties. Since the influenced factors are complex during the preparation, and few consensuses are reached for the structure and modification mechanism, relevant research should be further conducted.

In this study, hydroxy-titanium cations were introduced into the interlayer of montmorillonite by ion exchange, and titanium-pillared montmorillonite was obtained after calcination. Then, silane-modification was conducted in the solvents with different polarities, such as cyclohexane, anhydrous ethanol, and methanol. Finally, the effects of solvents and the formation mechanisms for these silylated products were discussed on the basis of the characterization of structure and morphology. This research is conducive to the application of montmorillonite for the removal of environmental pollutants and the synthesis of clay mineral-polymer nanocomposites.

2. EXPERIMENTAL SECTION

2.1. Materials

Ca-montmorillonite (Mt) used in this study was obtained from Inner Mongolia, China. γ-aminopropyltriethoxysilane (APTES) was purchased from Sigma-Aldrich (≥98%). Titanium (IV) isopropoxide was purchased from Sigma-Aldrich (≥95%). All reagents were of analytical grade and used.

2.2. Sample Preparation

2.2.1. Synthesis of Ti-Pillared Montmorillonite

Three grams of montmorillonite was dispersed in 150 mL isopropanol for 3 h, then 72 mL of titanium (IV) isopropoxide-isopropanol mixtures (17 v/v%) was added, followed by the dropwise addition of 100.5 mL of isopropanol and water mixture (60:40 v/v) under vigorous stirring at ambient temperature. After incubation for 2 h, the solid product was rinsed with isopropanol for three times, then separated by centrifugation and dried at 65 °C for 12 h. The powders were calcined at 400 °C for 4 h to obtain titanium-pillared montmorillonite (designated as Ti-Mt).

2.2.2. Silylation with APTES

Ten grams Ti-Mt and 5 mL APTES were mixed by stirring in 200 mL solvent, and then the mixture was refluxed at 105 °C for 20 h. The polar solvents used were ethanol and methanol, and the nonpolar solvents were cyclohexane. The silyated products were separated by centrifugation, washed with the solvent for six times, and then dried at 80 °C (designated as Ti-Mt-C-A, Ti-Mt-E-A, Ti-Mt-M-A for the products prepared in cyclohexane, ethanol and methanol, separately).

2.3. Characterization Method

X-ray diffraction (XRD) analysis was performed on an X-ray diffractometer (PANalytical EMPYREAN). The scanning range (2θ) was 0.5°–10°. Cu target was used. Scanning step is 0.013° step^{-1} and scan speed is 0.034° step^{-1}. Accelerating voltage is 40 kV with an accelerate current of 40 mA. The basal spacing was calculated from the 2θ values by Bragg equation.

FTIR spectra were collected on a Bruker VERTEX 70 Fourier transform infrared spectrometer. The scanning range is 400–4000 cm^{-1} with a resolution of 4 cm^{-1} and 64 scans.

Thermogravimetric analysis was performed on a NETZSCH STA 449 F3 Jupiter thermal analyzer in the temperature range of 40–1200 °C with a heating rate of 10 °C min^{-1} and flow velocity of high-purity argon as purge gas at 60 mL min^{-1}.

The specific surface areas of the different samples were determined by BET method from N_2 adsorption–desorption isotherms at 200 °C (Quantachrome iQ^2 Analyzer). The pore volume and pore size were calculated by BJH method. Before the adsorption measurement, the samples were evacuated at 200 °C under nitrogen gas for 20 h.

Morphology observation of the samples was performed in a FEI Scios scanning electron microscope (SEM) with an energy dispersive spectrometer. The powders were fixed on the holders with glue, and then purged with compressed air to remove the non-glued powders.

3. RESULTS AND DISCUSSION

3.1. XRD

Figure 1 shows the XRD patterns of the pristine montmorillonite, titanium pillared montmorillonite and silylated samples. The observed characteristic diffraction peak corresponds to the (001) lattice plane reflection of montmorillonite. The broad peak of the (001) reflection ($2\theta = 5.8°$, $d = 1.50$ nm) of Mt with weak intensity (Fig. 1(a)) underwent an obvious shift to smaller angles after titanium pillaring. The basal spacing for Ti-Mt is 11.46 nm (Fig. 1(b)), which suggests the existence of titanium oxides in the interlayer spaces. The estimated diameter of TiO_2 is 10.5 nm, which is calculated from the thickness of a single montmorillonite layer of 0.96 nm, and is accordance with the previous research.[24] The sharp diffraction peak of Ti-Mt (Fig. 2(b)) at 25.3° (2θ) displays a diffraction pattern characteristic of anatase.

By comparing silane-modified samples (Figs. 1(c–d)) with Ti-pillared montmorillonite, the broadening of the (001) reflection peak of Ti-Mt-C-A prepared in cyclohexane indicated the increase of amorphous contents in the modified sample. The interlayer distance decreased significantly. This could be caused by the structural collapse after a long time of reflux. For Ti-Mt-E-A and Ti-Mt-M-A (Figs. 1(d–e)), no distinguishable diffraction peaks were found.

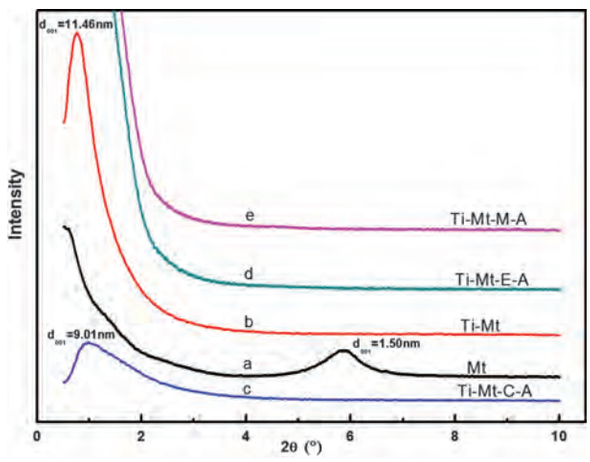

Figure 1. Small-angle XRD patterns of pristine Mt (a), Ti-Mt (b) and silylated Ti-Mt prepared in cyclohexane (c), ethanol (d), methanol (e).

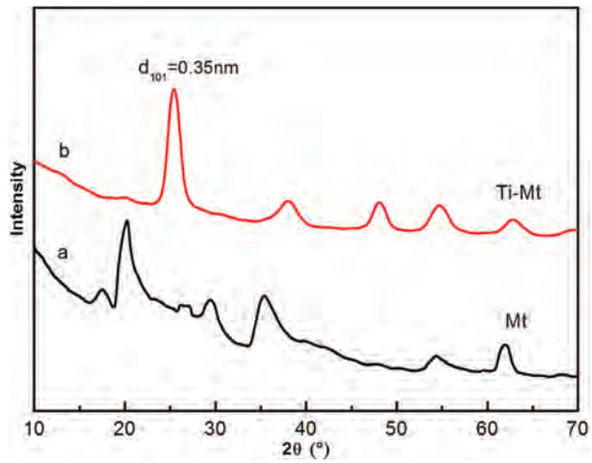

Figure 2. Wide-angle XRD patterns of pristine Mt (a), Ti-Mt (b).

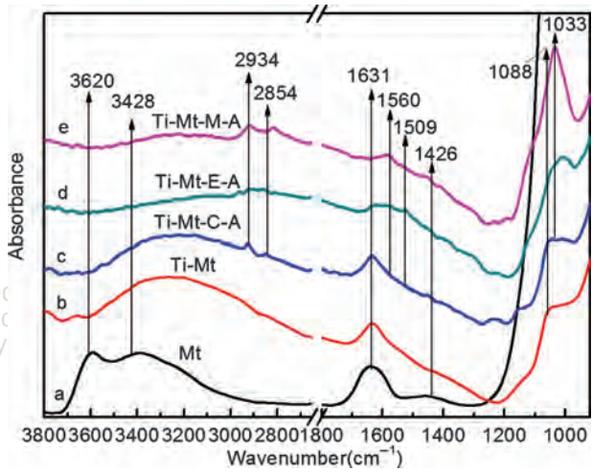

Figure 3. The FTIR patterns of the samples.

Table I. Positions and assignments of the main FTIR adsorption peaks.

Band position/cm^{-1}	Assignments	Band position/cm^{-1}	Assignments
3620	Al(Mg)–OH stretching of structure	1560	NH_2 bending
3428	O–H stretching of water	1509	CH_2 bending
2934	CH_2 asymmetric stretching	1426	CH_2 bending
2854	CH_2 symmetric stretching	1088	Si–O stretching
1631	H–O–H bending	1033	Si–O–Si stretching

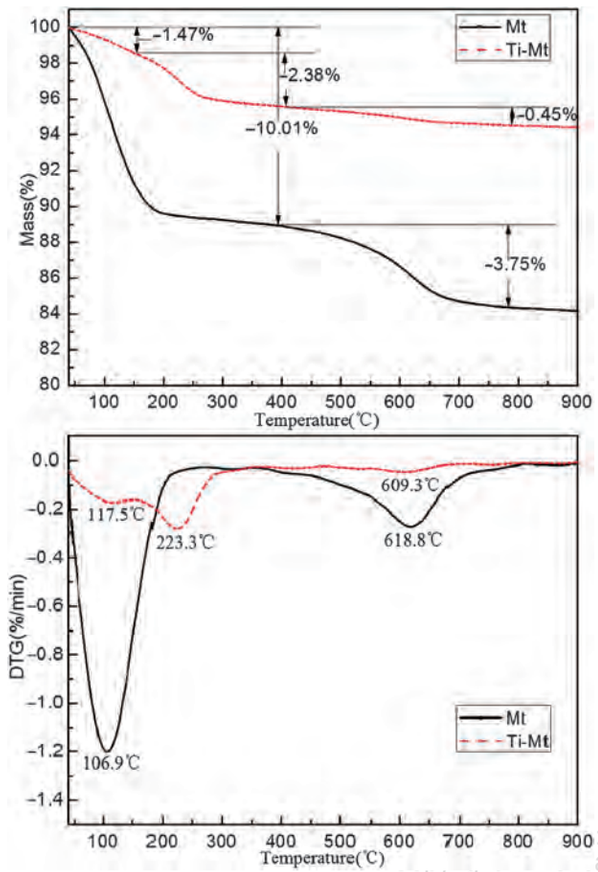

Figure 4. The TG/DTG patterns of the montmorillonite and the titanium pillared montmorillonite.

Table II. Mass losses of the montmorillonite, of titanium pillared montmorillonite samples in different temperature ranges.

Sample	40–400 °C	400–700 °C
Mt	10.01	3.75
Ti-Mt	3.85	0.45

Table III. Mass losses of the silylated samples between 300 and 500 °C.

Sample	Ti-Mt-C-A	Ti-Mt-E-A	Ti-Mt-M-A
W/%	1.72	4.12	4.59

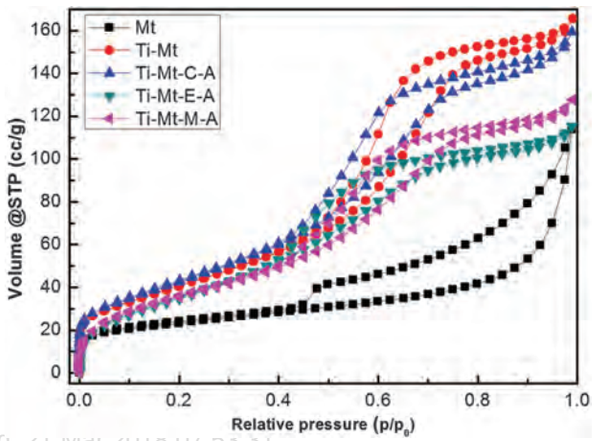

Figure 6. N_2 adsorption–desorption isotherms of montmorillonite, titanium-pillared montmorillonite and composite modified montmorillonite.

3.2. FTIR Spectra

The FTIR of samples were tested in order to further explore the bonding and loading of organic silane on Ti-pillared montmorillonite. The infrared spectra of the samples are shown in Figure 3. The positions and assignments of the infrared absorption peaks are shown in Table I.[25–27]

Compared with FTIR spectrum of the pristine montmorillonite (Fig. 3(a)), the intensity of the hydroxyl stretching vibration of Al(Mg)–OH at ca. 3620 cm^{-1} and that of water at ca. 3428 cm^{-1} diminished for Ti-Mt (Fig. 3(b)), which is caused by the dehydration and dehydroxylation during calcination. The intensities of the peaks among 1000–1200 cm^{-1} significantly decreased after titanium

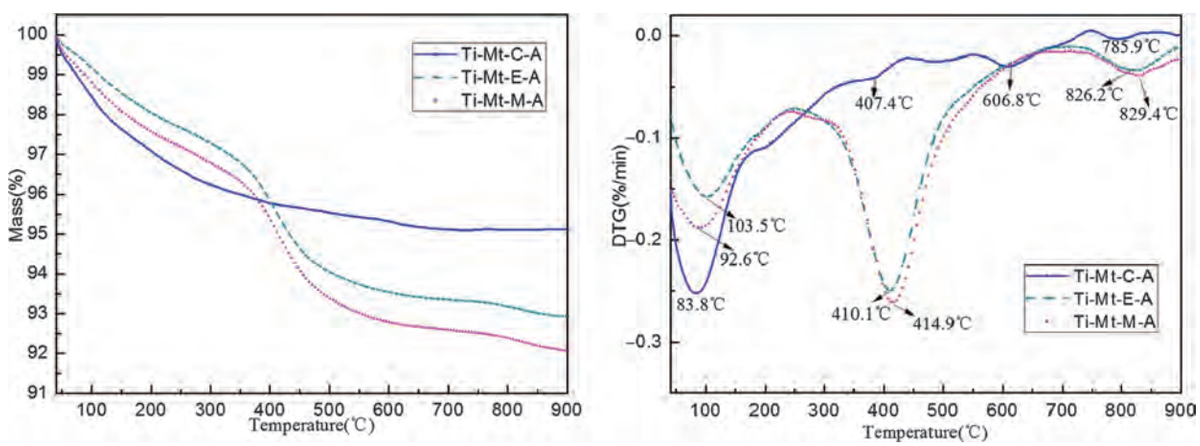

Figure 5. The TG/DTG patterns of the APTES modified samples.

Table IV. Specific surface area, pore size and pore volume of montmorillonite, titanium-pillared montmorillonite and composite modified montmorillonite.

Sample	S_{BET}/(m^2/g)	D_{BJH} (nm)	V_{BJH} (cc/g)
Mt	79.49	3.13	0.15
Ti-Mt	152.45	5.80	0.25
Ti-Mt-C-A	150.99	5.41	0.24
Ti-Mt-E-A	148.19	3.71	0.18
Ti-Mt-M-A	130.14	4.44	0.19

pillaring, because many titanium oxides occupied the interlayer space, which reduce the proportion of SiO_2 content in the titanium-pillared samples.

In the FTIR spectra of the silylated products (Figs. 3(c–e)), several new adsorption peaks emerged. These provided supporting evidence for the existence of APTES in the surfaces of montmorillonite. The vibration at 2934 cm^{-1} and 2854 cm^{-1} are attributed to the asymmetric and symmetric stretching vibration of $–CH_2$, the bending vibration of $–NH_2$ at ca. 1560 cm^{-1} and the deformation vibration of $–CH_2$ at ca. 1509 cm^{-1}.[21, 29] The decrease of –OH vibration, a frequency shift of the vibration from 1088 cm^{-1} (Si–O vibration) to 1033 cm^{-1} (Si–O–Si vibration) and the sharpening of Si–O–Si vibration peaks with the increase of solvent polarity are all proof of the bonding of APTES with montmorillonite.[28] According to the IR spectra, the sequence of the silane loading amounts is Ti-Mt-M-A > Ti-Mt-E-A > Ti-Mt-C-A.

3.3. Thermal Analysis

Thermogravimetric analysis provided a simple and effective way for measuring the amount of loaded silane and the different types of water in the samples. The TG/DTG curves of the samples without and with silylation are shown in Figures 4 and 5, respectively.

For pristine montmorillonite (Mt) and titanium pillared montmorillonite (Ti-Mt), the mass losses below 400 °C were caused by the evaporation of water adsorbed on the surface and interlayer space of the samples (Fig. 4, and Table II). The dehydration process of Ti-Mt lasts for a longer period than that of Mt, since the diverse pore structure of Ti-Mt restrained the escape of water molecules. The mass loss between 40–400 °C is 3.85% for Ti-Mt, which is much less than 10.01% for Mt. This is the result of

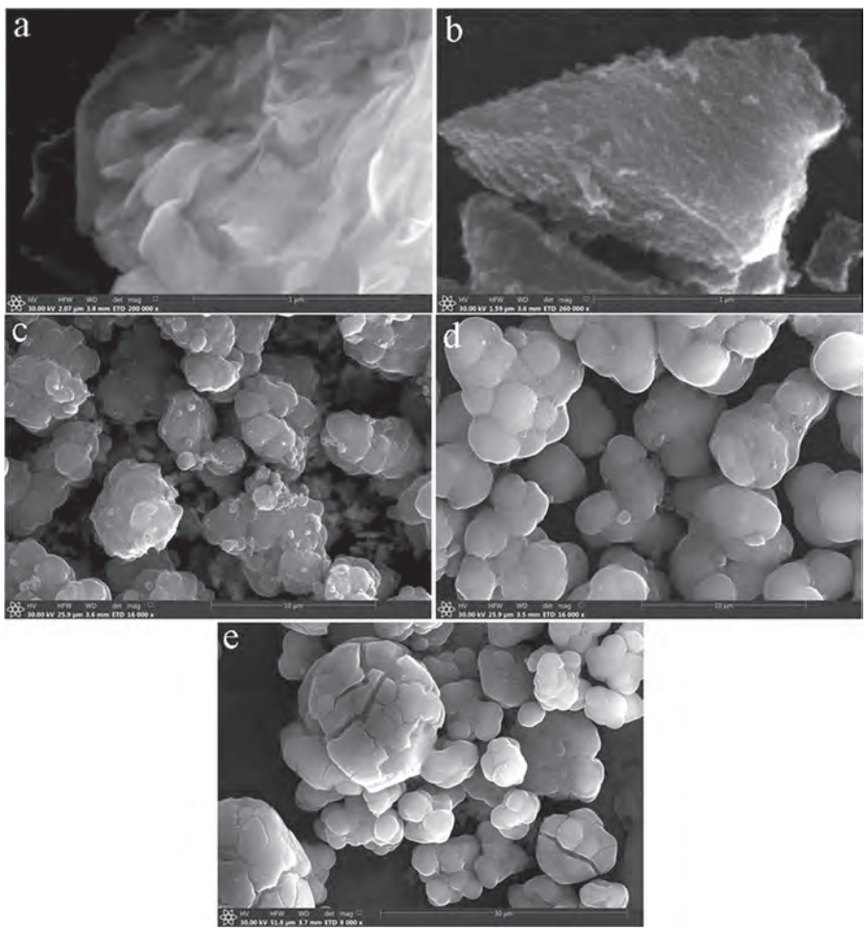

Figure 7. SEM images of the samples with/without modification. (a) Mt; (b) Ti-Mt; (c) Ti-Mt-C-A; (d) Ti-Mt-E-A; (e) Ti-Mt-M-A.

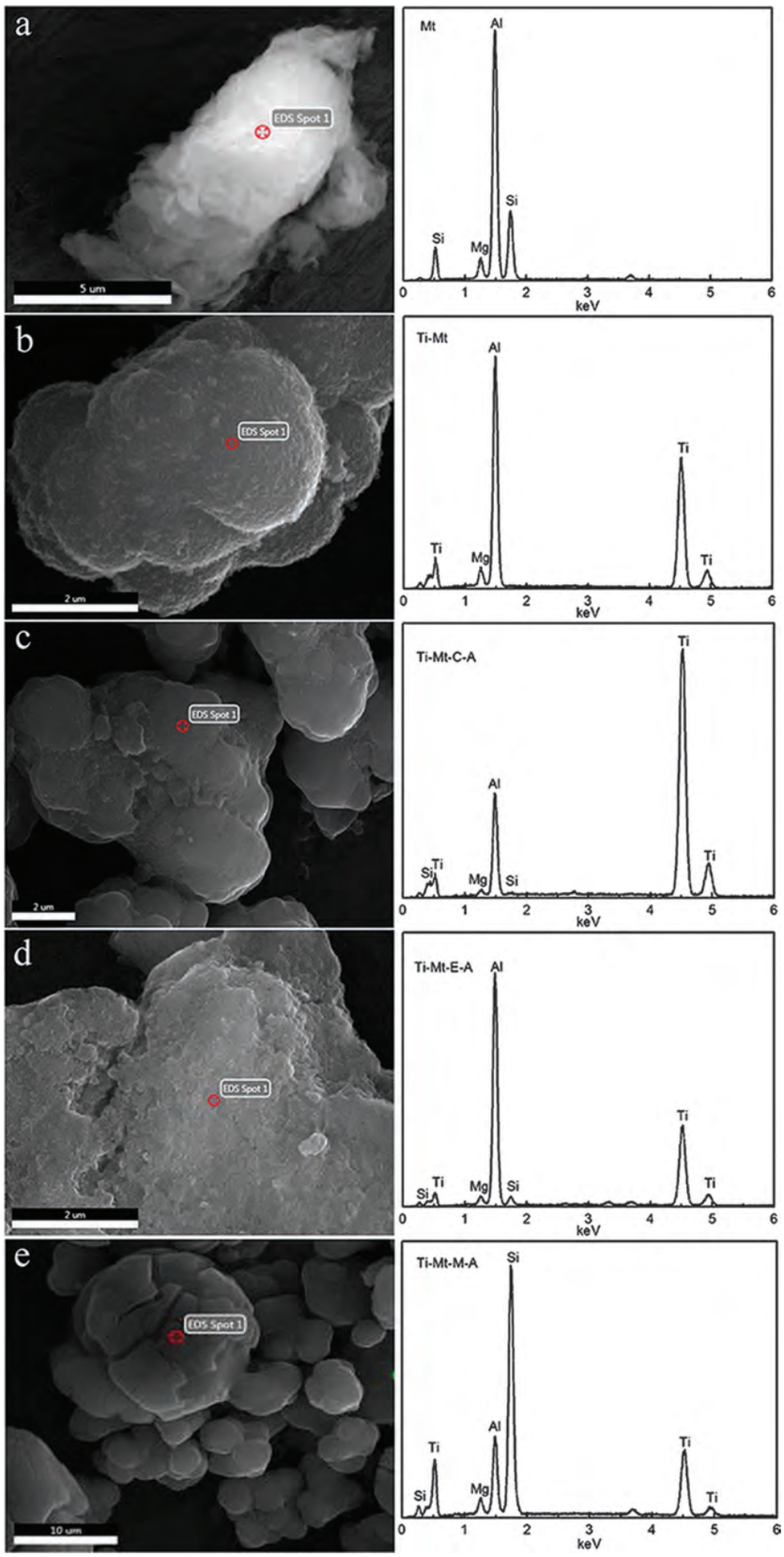

Figure 8. SEM and EDS images of the samples with/without modification.

intercalation and calcination, which has removed most of the physical adsorbed water and interlayer water. The DTG peaks emerging at about 610 °C are caused by dehydroxylation. During 400–700 °C, the mass loss of Ti-Mt (0.45%) is significantly less than that of Mt (3.75%), which indicates the pillaring process would decrease the amounts of hydroxyl in Ti-Mt. This is also evidence that the interlayer substance is titanium oxide rather than a hydroxyl compound.

Figure 5 is the TG/DTG curves of silane-modified samples. Most of the modified products have three peaks of mass loss. The peaks at about 100 °C are mainly caused by desorption of solvent molecules, as well as by a small amount of physical adsorbed and interlayer water. The mass loss above 600 °C is due to the depletion of hydroxyls.[18,28] The DTG peak near 410 °C resulted from the decomposition of the ethoxyl groups in organic silane.[25] The mass losses of the silane modified samples between 300–500 °C are shown in Table III. Ti-Mt-M-A has the highest loading amount of silane, which is consistent with the results of FTIR analysis.

3.4. Specific Surface Area, Pore Size and Pore Volume

The N_2 adsorption–desorption isotherms of all samples is of type IV with hysteresis loops (Fig. 6) indicating the mesoporous structures.[29,30]

The BET specific surface area of pristine montmorillonite is 79.49 m^2/g and the pore diameter is 3.13 nm. After pillaring, the numbers were both nearly doubled (152.45 m^2/g and 5.80 nm for Ti-Mt). Titanium pillaring can significantly increase the specific surface area and pore size, which is in accordance with the results of XRD.

The specific surface areas of Ti-Mt-C-A, Ti-Mt-E-A, and Ti-Mt-M-A are 150.99 m^2/g, 148.19 m^2/g, and 130.14 m^2/g, respectively (Table IV). Compared with Ti-Mt, there is a decrease for these silylated samples, since the silane occupied some pore structure. Furthermore, the little decrease indicated that the silane modifications in these solvents retain the original pore structure of titanium pillared montmorillonite well. Ti-Mt-C-A that was prepared in cyclohexane possess the largest specific surface area, pore size and pore volume, since it has the lowest loading amounts of silane. The samples prepared in ethanol and methanol have relatively low specific surface area and pore volume, because the APTES molecules fill the mesoporous structure of titanium pillared montmorillonite, hindering the N_2 access into the channel of titanium pillared montmorillonite.[31,32] These results also demonstrate the high silane loading of Ti-Mt-M-A in agreement with the infrared spectra and the thermal analyses.

3.5. SEM

The pristine montmorillonite consist of "corn flake-looking" particles from the SEM image in Figure 7(a).[27] After titanium pillaring, the stacking of layers become more regular (Fig. 7(b)). Combined with the results of EDS (Fig. 8) and XRD, this suggests that the final product is titanium pillared montmorillonite rather than a mixture of titanium oxides and montmorillonite particles, since no particles that contain titanium without aluminum and silicon are found. The samples with APTES modification present a chip-shape. Some cracks occurred on the surface of Ti-Mt-M-A, because more APTES molecules are loaded in this sample, and the montmorillonite was encapsulated by the silanes. The silane layer breaks during the drying of this sample.

3.6. Grafting Mechanism

According to the results that we obtained and the mechanisms proposed by Day et al.,[33] the potential processes that occurred between the silane and the titanium-pillared montmorillonite in different solvents were proposed in Figure 9. Since calcination removes most of the physically adsorbed water in titanium pillared montmorillonite, the hydrolysis of APTES was significantly controlled by the behaviors of the few water molecules in the different solvents, thus affecting the silane loading amounts.[34]

The experimental results show that the alcohol system is more effective to the silane-grafting process. Alcohol can form ethoxides on the surface of titanium oxide by means of replacing the surface water molecules on the titanium oxide (Fig. 9(b)), which increases the concentration of water in the system to promote the APTES hydrolysis. The diffusion efficiency of water molecules in the alcohol system is much better than that in cyclohexane; thus, the silanol molecules are easier to form and more accessible to reactive sites on pillared montmorillonite.[35] However, the water molecules tend to enter the interlayer channel of titanium pillared montmorillonite in the cyclohexane system due to the molecular repulsion between water and cyclohexane, which can greatly reduce the exposure of APTES with water molecules, causing the hydrolysis reaction to be more difficult to carry on. Thus, fewer loading amounts of silane exist in the final products prepared in cyclohexane.

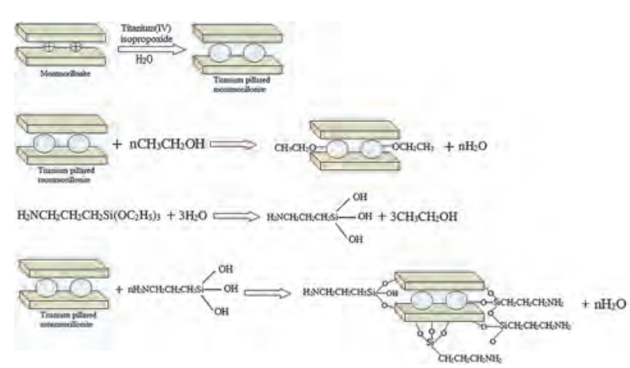

Figure 9. Schematic representation of the reactions between the titanium pillared montmorillonite and the alkoxysilanes.

4. CONCLUSION

Titanium pillared montmorillonite was modified with γ-aminopropyltriethoxysilane (APTES) in different solvents. The results show that titanium pillared montmorillonite with attached APTES in interlayer surface was prepared successfully. The methanol system is more conducive to the silane-grafting process, and the products possess a high loading amount of APTES. Alcohol could increase the possibility that APTES contact with water will promote the grafting reaction between APTES and titanium pillared montmorillonite. However, the water molecules tend to enter the interlayer channel of the pillared montmorillonite in the cyclohexane system and are difficult to contact with silane due to the molecular repulsion. Therefore it is unbeneficial to silylation in cycohexane. These results suggest that the solvent used has an important influence on the structure and grafting mechanism of the silylated products. Therefore, the silane loading amount could be controlled by choosing an appropriate solvent. These composites have broadened prospects in the future of environmental pollutants and the preparation of clay mineral-polymer nanocomposites.

Acknowledgment: This work was financially supported by the National Natural Science Foundation of China (Grant No. 41202031) and the West Light Foundation of the Chinese Academy of Sciences.

References and Notes

1. S. Babel and T. A. Kurniawan, *J. Hazard. Mater.* 97, 219 (**2003**).
2. K. Y. Wang, Y. M. Chen, and Y. Zhang, *Polymer.* 49, 3301 (**2008**).
3. D. Y. Wang, J. Zhu, Q. Yao, and C. A. Wikie, *Chem. Mater.* 14, 3837 (**2002**).
4. S. S. Ray and M. Okamoto, *Prog. Polym. Sci.* 28, 1539 (**2003**).
5. S. Pavlidou and C. D. Papaspyrides, *Prog. Polym. Sci.* 33, 1119 (**2008**).
6. Y. F. Xi, D. Zhe, H. P. He, and R. L. Frost, *J. Colloid Interface Sci.* 277, 116 (**2004**).
7. J. N. Ding, Y. G. Meng, and S. Z. Wen, *J. Adhes.* 78, 645 (**2002**).
8. C. Breen, R. Watson, J. Madejová, A. P. Komadel, and Z. Klapyta, *Langmuir: The ACS Journal of Surfaces and Colloids* 13, 6473 (**1997**).
9. S. K. Dentel, J. Y. Bottero, K. Khatib, H. Demougeot, J. P. Duguet, and C. Anselme, *Water Res.* 29, 1273 (**1995**).
10. E. Eren and B. Afsin, *Dyes and Pigments* 76, 220 (**2008**).
11. S. H. Lin and R. S. Juang, *J. Hazard. Mater.* 92, 315 (**2002**).
12. J. T. Kloprogge, *J. Porous Mater.* 5, 5 (**1997**).
13. E. Manias, A. Touny, L. Wu, K. Strawhecker, A. B. Lu, and T. C. Chung, *Chem. Mater.* 13, 3516 (**2001**).
14. J. Lemić, M. Djuričić, and T. Stanić, *J. Colloid Interface Sci.* 292, 11 (**2005**).
15. L. Beaudet, K. Z. Hossain, and L. Mercier, *Chem. Mater.* 15, 327 (**2002**).
16. D. Gournis, V. Georgakilas, M. A. Karakassides, T. Bakas, K. Kordatos, M. Prato, M. Fanti, and F. Zerbetto, *J. Am. Chem. Soc.* 126, 8561 (**2004**).
17. N. N. Herrera, *J. Mater. Chem.* 15, 863 (**2005**).
18. F. Piscitelli, P. Posocco, R. Toth, M. Fermeglia, S. Pricl, G. Mensitieri, and M. Lavorgna, *J. Colloid Interface Sci.* 351, 108 (**2010**).
19. H. P. He, Q. Tao, J. X. Zhu, P. Yuan, W. Shen, and S. Q. Yang, *Appl. Clay Sci.* 71, 15 (**2013**).
20. A. M. Shanmugharaj, K. Y. Rhee, and S. H. Ryu, *J. Colloid Interface Sci.* 298, 854 (**2006**).
21. L. N. Su, T. Qi, H. P. He, J. Zhu, P. Yuan, and R. Zhu, *J. Colloid Interface Sci.* 391, 16 (**2013**).
22. J. F. Li, Y. M. Li, and J. H. Lu, *Appl. Clay Sci.* 46, 314 (**2009**).
23. S. Al-Asheh, F. Banat, and L. Abu-Aitah, *Sep. Purif. Technol.* 33, 1 (**2003**).
24. K. Mogyorosi, I. Dekany, and J. H. Fendler, *Langmuir: The ACS Journal of Surfaces and Colloids* 19, 188 (**2003**).
25. H. P. He, J. Duchet, J. Galy, and J. F. Gerard, *J. Colloid Interface Sci.* 288, 171 (**2005**).
26. J. Madejova, *Vib. Spectrosc.* 31, 1 (**2003**).
27. Y. H. Ma, J. X. Zhu, H. He, P. Yuan, W. Shen, and D. Liu, *Spectrochimica Acta Part A Molecular and Biomolecular Spectroscopy* 76, 122 (**2010**).
28. W. Shen, H. P. He, J. X. Zhu, P. Yuan, and R. L. Frost, *J. Colloid Interface Sci.* 313, 268 (**2007**).
29. J. Rouquerol, F. Rouquerol, P. Llewellyn, G. Maurin, and K. S. W. Sing, *Adsorption by Powders and Porous Solids (Second Edition)* (**2012**).
30. K. M. S. Khalil, T. Baird, M. I. Zaki, A. A. El-Samahy, and A. M. Awad, *Colloid Surf. A-Physicochem. Eng. Asp.* 132, 31 (**1998**).
31. K. S. W. Sing, D. H. Everett, R. A. W. Haul, L. Moscou, R. A. Pierotti, J. Rouquerol, and T. Siemieniewska, *Reporting Physisorption Data for Gas/Solid Systems* (**2008**).
32. P. X. Wu, Y. P. Dai, H. Long, N. W. Zhu, P. Li, J. H. Wu, and Z. Dang, *Chem. Eng. J.* 191, 288 (**2012**).
33. R. Day, G. Parfitt, and J. Peacock, *Discussions of the Faraday Society* 52, 215 (**1971**).
34. A. D. Gianni, E. Amerio, O. Monticelli, and R. Bongiovanni, *Appl. Clay Sci.* 42, 116 (**2008**).
35. K. W. Park and O. Y. Kwon, *Bull. Korean Chem. Soc.* 25, 965 (**2004**).

Received: 17 March 2016. Accepted: 12 September 2016.